Iron-Loss Model With Consideration of Minor Loops Applied to FE-Simulations of Electrical Machines

Simon Steentjes, Georg von Pfingsten, Marco Hombitzer, and Kay Hameyer

Institute of Electrical Machines, RWTH Aachen University, Germany

The accurate prediction of iron losses in soft magnetic materials for various frequencies and magnetic flux densities is eminent for an enhanced design of electrical machines in automotive applications. For this purpose different phenomenological iron-loss models have been proposed describing the loss generating effects. Most of these suffer from poor accuracy for high frequencies as well as high values of magnetic flux densities. This paper presents an advanced iron-loss formula, the IEM-Formula, which resolves the limitation of the common iron-loss models by introducing a high order term of the magnetic flux density. Furthermore the IEM-Formula is extended in order to include the influence of higher harmonics as well as minor loops. In line with this a detailed study of minor loop loss behavior is presented. Exemplarily, the iron-loss formula is utilized to calculate the iron losses of a permanent magnet synchronous machine for the drive train of a full electric vehicle.

***Index Terms*—Eddy current losses, hysteresis, iron losses, magnetic saturation effects, minor loops,.**

I. Introduction

In general the design process of an electrical machine is based on analytical preliminary calculation of the electromagnetic circuit followed by FE-simulations for refinement. For an accurate design knowledge regarding soft magnetic material's behavior at various operating points is eminent. This includes the material's magnetizability and in particular the estimation of the iron losses caused by alternating magnetic flux in the rotor and stator material.

Accurate iron-loss estimation is essential in order to achieve a high efficiency and an advantageous utilization of the soft magnetic material in electrical machines, i.e., power density.

The iron losses are calculated in a post-process of solutions of FE-simulations. The transient FE-simulation generates for each finite element output data of the flux density in each time step. Based on these data the resulting time dependent magnetic flux density is derived. The iron-loss model requires such data to compute the iron losses.

Common empirical loss models are sufficiently accurate for low flux densities and frequencies, often neglecting the harmonics in magnetic flux and other parasitic effects. Therefore, these models are not suitable for highly saturated materials, higher harmonics, and frequencies above 400 Hz [1], [2]. Electrical machines for e.g., traction motors in automotive application can operate in the range of $1.3\ \mathrm{T} \leq B \leq 2.0\ \mathrm{T}$ for the flux densities and magnetization frequencies $f \geq 400$ Hz. To match such conditions, the IEM recently developed a 5-parameter-formula [1], [2].

In this paper, the consideration of arbitrary magnetic flux density waveforms and minor loops is studied. A detailed analysis of the influence of harmonics and the resulting minor loops on the iron-losses at various frequencies and flux density amplitudes is performed. Particular attention is paid to the influence of the phase angle of the higher harmonics on the iron losses. As a consequence, a commonly used empirical formula for minor loop loss calculation [3] is evaluated.

The aforementioned effects are included in the IEM-Formula, which is finally applied to calculate the losses in an example of a permanent magnet synchronous machine. The predicted loss values are compared to measurements.

II. The IEM-Formula

It has been determined in [1], [2], and [4] that the classical Bertotti model [5] underestimates losses at high magnetic flux densities and high frequencies due to neglecting saturation. To overcome this, the IEM proposed and validated a fourth loss term with a higher order B dependence (which means higher than B^2 for the classical Foucault eddy current losses).

The proposed mathematical formulation with higher order B term reads as follows:

$$P_{\mathrm{IEM}} = a_1 \hat{B}^{\alpha} f + a_2 \hat{B}^2 f^2 (1 + a_3 \hat{B}^{a_4}) + a_5 \hat{B}^{1.5} f^{1.5} \quad (1)$$

where:

- $\hat{B}$: magnetic flux density in Tesla [T];
- f: fundamental frequency in Hertz [Hz];
- a_{i}, α: fitted material parameters

Hysteresis losses, classical Foucault eddy current losses and excess losses are included (respectively as terms with a_1, a_2 and a_5 coefficients), as well as the additional higher order term $a_3 \hat{B}^{a_4}$.

The proposed loss model is based on the fundamental frequency component and the a-parameters are identified following a semiphysical identification procedure using standardized Epstein measurements (Section III).

III. Parameter Identification

The parameters a_1–a_5 used in (1) are identified by a semiphysical identification procedure [2]. Measurements are performed at a standard Epstein Frame with sinusoidal uniaxial magnetic flux densities on 24 stripes of soft magnetic material with dimensions of 280 mm × 30 mm. The stripes are uniformly distributed in accordance with the rolling direction using 12 stripes along and 12 stripes perpendicular to the rolling direction.

Manuscript received November 05, 2012; revised January 23, 2013; accepted January 23, 2013. Date of current version July 15, 2013. Corresponding author: S. Steentjes (e-mail: Simon.Steentjes@iem.rwth-aachen.de).

Color versions of one or more of the figures in this paper are available online at http://ieeexplore.ieee.org.

Digital Object Identifier 10.1109/TMAG.2013.2244072

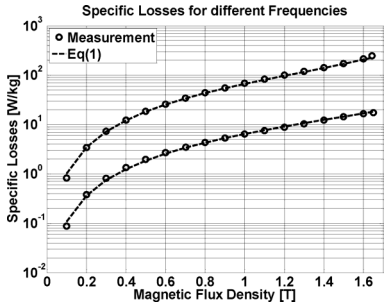

Fig. 1. Comparison of the 5-Parameter-IEM-Formula (1) with measurements at frequencies of 200 Hz (low) and 1000 Hz (top), employing the parameter set of a typical NO FeSi material collected in Table I.

TABLE I
IDENTIFIED PARAMETERS FOR THE INVESTIGATED NO MATERIAL

α	a_1	a_2
1.801	$20.322 \cdot 10^{-3}$	$34.648 \cdot 10^{-6}$
a_3	a_4	a_5
$30.489 \cdot 10^{-3}$	6.149	$0.340 \cdot 10^{-3}$

The semiphysical identification process to determine the parameters a_1 and α is performed by dc-measurements (quasi-static loss measurements using a flux-meter) at a standard Epstein frame, finding the best parameter set describing the hysteresis losses

$$E_{\mathrm{DC}} = a_1 \cdot \hat{B}^{\alpha}. \tag{2}$$

The parameter a_2, correlating with the classical Foucault eddy current losses, is calculated by the macroscopic equation obtained from Maxwell's equations

$$a_2 = \frac{\pi^2 d^2}{6 \rho \rho_e} \tag{3}$$

with sheet thickness d, specific density ρ and specific electrical resistivity ρ_{e} of the soft magnetic material.

The excess loss parameter a_5 is identified by measurements at rather low magnetic flux densities and frequencies between 5 Hz and 10 Hz. Saturation losses can be neglected at this point and the excess loss term is separated from measurements by subtraction of the preliminary described hysteresis (2) and classical Foucault eddy current losses (3).

Parameters a_3 and a_4 are determined from the nonlinear material behavior at high frequencies and magnetic flux densities [2].

Table I presents the parameters obtained by using the semiphysical identification procedure for a nonoriented FeSi 3% electrical steel sheet. Employing the determined parameters, the predicted iron losses by the IEM-Formula (1) are compared to measurements (see Fig. 1). The comparison shows a very good accordance.

IV. MINOR LOOPS AND HARMONICS

Magnetic flux paths occurring in rotating electrical machines are more complicated than in the case of standardized material characterization of the Epstein-strips (i.e., unidirectional and sinusoidal magnetic flux density). However, the actual iron losses occurring in electrical machines cannot be placed in a simple relationship to the Epstein loss data.

These limitations emphasize the need to expand the existing loss approach further to describe the harmonics of the magnetic flux density waveform due to iron saturation, skin effect, stator and rotor slots, harmonics in excitation and supply currents (e.g., pulse-width modulation) in the iron-loss calculation to more accurately predict the iron losses.

According to [6], [7], the influence of harmonics (i.e., in general various degrees of distortion in grain-oriented, nonoriented, and amorphous laminations) can be included in an analytical expression extending the iron-loss formula (1) to generic flux waveforms by a Fourier-analysis.

Hence, the classical Foucault eddy current loss term as well as the excess loss term is expanded by a summation over all harmonics in order to take the influences of harmonics into account. The hysteresis loss component remains unchanged. This procedure yields an implicit equation, which can be easily computed.

The discussed extensions are sufficient for those cases where no minor loops occur. However, depending on the magnitude and phase of the magnetic flux density harmonics specified, the resulting magnetic flux density waveform may contain flux density reversals, leading to so-called minor loops. In such cases the hysteresis losses will vary with distortion. Several factors influence the magnitude of the flux density reversals and subsequently the minor loop losses. The most important ones are the harmonics' phase angle and the order of the harmonic components. In addition the premagnetization has to be taken into account (i.e., the magnetization state of the material).

Commonly empirical correction factors assuming a linear dependence between the minor hysteresis loop losses and the minor loop modulation (ΔB) are employed [3], [8]. This transforms the hysteresis loss contribution of (1) from $P_{\mathrm{hy}} = a_1 \cdot \hat{B}^{\alpha} \cdot f$ to

$$P_{\mathrm{hy}} = \left(1 + k \cdot \left(\frac{1}{\hat{B}} \cdot \sum_{n=1}^{N} \Delta B_n\right)\right) \cdot a_1 \cdot \hat{B}^{\alpha} \cdot f, \tag{4}$$

with N the amount of flux density reversals and k a material dependent correction factor. Such correction factors result in unsatisfactory results (Fig. 3) and alternative approaches need to be studied. Therefore, measurements at different magnetic flux density values and different frequencies are conducted with a varying phase angle between 0° and 180° (Fig. 2). Using these measurements, the minor loop areas, i.e., the minor loop losses, can be computed analytically. Fig. 3 presents the predicted iron losses assuming a linear dependence between minor loop loss and modulation as in (4) referenced to the measured iron losses. This result underlines the insufficient and inaccurate loss estimation by the common empirical correction factors based on a linear correlation.

A similar approach as for the discussed case of the classical Foucault eddy current and excess losses is now adapted. This approach is based on a ΔB^{α} dependence, yielding a good accuracy despite its empirical origin (Fig. 4).

Finally, the incorporation of the aforementioned effects leads to the following extended IEM-formula:

$$P_{\mathrm{IEM}}(\hat{B}, f) = P_{\mathrm{hy}}(\hat{B}, f) + P_{\mathrm{cl}}(\hat{B}, f) + P_{\mathrm{exc}}(\hat{B}, f) + P_{\mathrm{sat}}(\hat{B}, f) \tag{5}$$

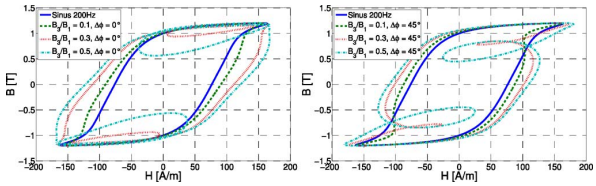

Fig. 2. Influence of the phase angle and the modulation ratio on the minor hysteresis loop: $\Delta\phi = 0°$ (above) and $\Delta\phi = 45°$ (below) for a typical NO FeSi 3.2% material.

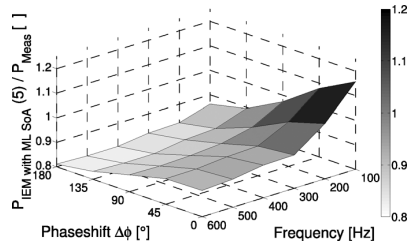

Fig. 3. Comparison of iron loss prediction assuming a linear relation between minor hysteresis loop loss and modulation ΔB [8], [9] for a typical NO FeSi 3.2% material.

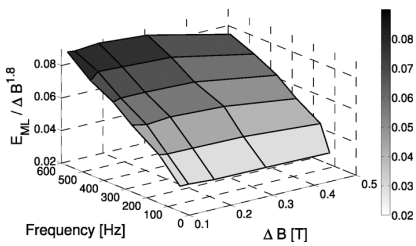

Fig. 4. Ratio between minor loop area E_{ML} and ΔB^{α} ($\alpha = 1.8$) for a typical NO FeSi 3.2% material.

with the following contributions:

$$P_{\mathrm{hy}}(\hat{B}, f) = a_1 \cdot \sum_{\mathrm{n}=0}^{\infty} \left(\hat{B}_{\mathrm{n}}^{\alpha} \cdot f_{\mathrm{n}} \right) \tag{6}$$

$$P_{\mathrm{cl}}(\hat{B}, f) = a_2 \cdot \sum_{\mathrm{n}=0}^{\infty} \left(\hat{B}_{\mathrm{n}}^{2} \cdot f_{\mathrm{n}}^{2} \right) \tag{7}$$

$$P_{\mathrm{exc}}(\hat{B}, f) = a_5 \cdot \sum_{\mathrm{n}=0}^{\infty} \left(\hat{B}_{\mathrm{n}}^{0.75} \cdot f_{\mathrm{n}}^{0.75} \right)^2 \tag{8}$$

$$P_{\mathrm{sat}}(\hat{B}, f) = a_2 \cdot a_3 \cdot \hat{B}^{a_4+2} \cdot f^2 \tag{9}$$

By employing a FFT on the flux density, the phase-shift $\Delta\varphi$ between the harmonics and the fundamental frequency is taken into account by analyzing the resulting flux density over one electrical period.

Subsequently the IEM-Formula is compared to nonstandard measurements, i.e., measurements with harmonic contents imposed in the magnetic flux density waveform. The used parameter set consists of the one, identified under sinusoidal uniaxial magnetic flux density conditions (Table I). The Epstein measurement results correspond with the nonsinusoidal magnetic flux density waveform. On the other hand, the IEM-Formula (5) is applied to these conditions by the given data for the harmonics' frequencies and magnitudes, giving rise to a calculated iron-loss value, which then can be compared to the experimental data. With this method the accuracy and reasonability of the model extensions for higher harmonics and minor loops in the IEM-Formula are studied in detail. The presented resulting

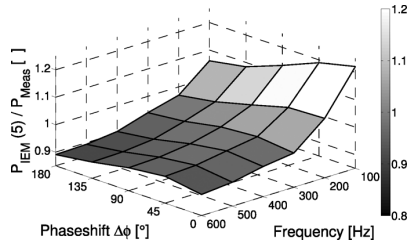

Fig. 5. Comparison of iron loss prediction using (5) and measured iron losses for a typical NO FeSi 3.2% material.

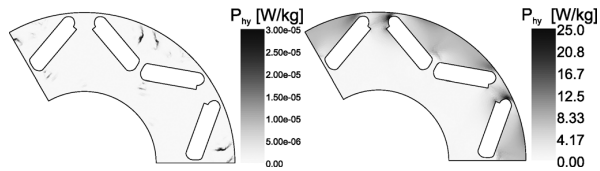

Fig. 6. Hysteresis loss distribution without (left) and with consideration of minor hysteresis loops (right).

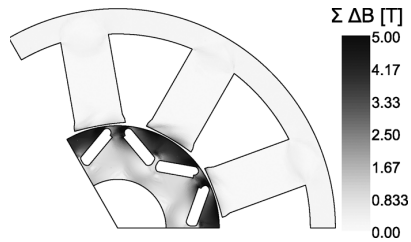

Fig. 7. Sum of the flux density reversals ΔB, i.e., minor loop amplitudes, in the stator and rotor core during one electrical period.

losses for different flux density waveforms, calculated as well as measured, emphasize the accuracy of the developed loss model (Fig. 5).

V. Permanent-Magnet Machine Analysis

The IEM-Formula (5) is exemplarily employed to a permanent magnetic synchronous machine (PSM) with a permanently deliverable torque of 80 Nm. The cross section of the laminated stator and rotor core of the six pole PSM under study is shown in Figs. 6(left) and 7. The maximum rotational speed of the machine is 18.000 rpm with a transition speed of 7.000 rpm. A concentrated winding is used to generate the six pole airgap field. The rotor of the investigated machine is excited by V-shaped buried magnets (Fig. 6).

Single-valued magnetization curves have been used to consider saturation effects originating from the nonlinear material behavior. The magnetic material is utilized up to 2 T in the considered machine. Second-order effects, originating from hysteresis behavior, are neglected.

A minor loop detection scheme is developed. Only minor loop losses are calculated when they actually occur. A consideration of minor loops is in the examined machine particularly relevant on the rotor side (Figs. 6(right) and 7). Above the permanent magnets, the number of flux reversals is greatest, resulting in significant minor hysteresis loop losses. Neglecting the minor loop hysteresis losses leads to a significant underestimation of the rotor losses (Fig. 6(left)). The contributions appearing in Fig. 6(left) are related to numerical noise. Overall, the hysteresis losses in the rotor take 50% of the total rotor losses.

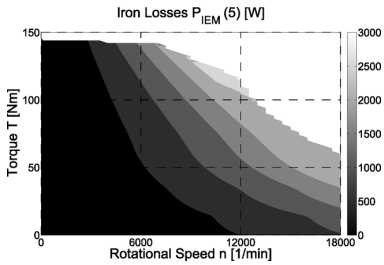

Fig. 8. Total iron losses predicted by (5).

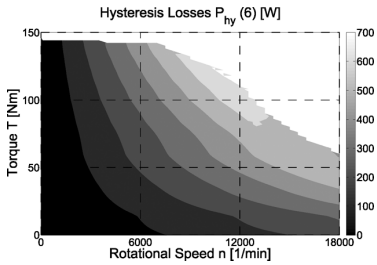

Fig. 9. Hysteresis loss contribution using (6).

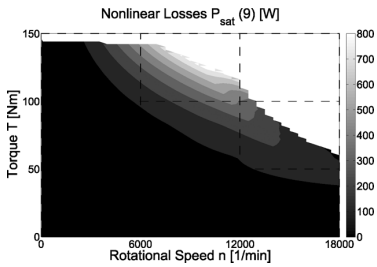

Fig. 10. Non-linear (saturation) loss contribution using (9).

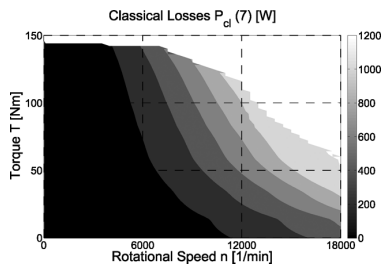

Fig. 11. Eddy current loss contribution using (7).

Pure hysteresis losses including minor loops, classical Foucault eddy current, excess as well as saturation losses in the laminated stator and rotor cores are estimated a-posteriori using the local waveforms of the magnetic flux densities in (5) (Figs. 8–12). Hysteresis losses (Fig. 9) play an important role over the whole speed-torque range, in particular at low speeds. Furthermore, a significant increase of hysteresis losses in the field-weakening range, especially in the range after passing through the transition point, is evident. The nonlinear loss component (9) has particularly in the area around the transition point (i.e., at high torques and high speeds) a large proportion. In contrast, the classical

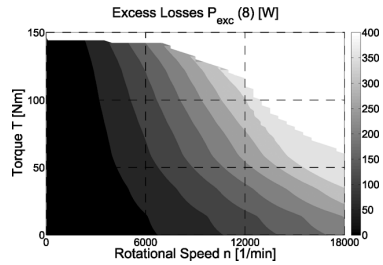

Fig. 12. Excess loss contribution using (8).

Foucault eddy current (7) and excess losses (8) are at high frequencies over a wide range of torque of importance.

VI. Conclusion

This paper presents a modified iron-loss model for the accurate iron-loss estimation under realistic and nonideal magnetization conditions. The model considers harmonics as well as the influence of minor hysteresis loops and saturation effects up to high frequencies—1500 Hz—and flux densities -1.7 T. The accuracy of the computed iron losses for harmonics under saturation is shown by the comparison of simulations to measurements under nonsinusoidal excitations at an Epstein frame. Commonly used iron-loss models are insufficient at high magnetic flux densities and frequencies, resulting in the need for advanced iron-loss formulas. Such improved iron-loss estimation is indispensable for increasing the machine performance and efficiency. As a consequence, this approach forms the basis for selecting the most appropriate electrical steel grade which suits best the specific working conditions in rotating electrical machines and gives insight in the specific trade-offs that are made during the machine design process. Particular requirements on electrical steel for specific applications can be identified for further steel development.

References

[1] D. Schmidt, M. van der Giet, and K. Hameyer, "Improved iron-loss prediction by a modified loss-equation using a reduced parameter identification range," in *Proc. Conf. 20th Int. Conf. Soft Magn. Mater.SMM20*, Kos, Greece, 2011, p. 421.

[2] D. Eggers, S. Steentjes, and K. Hameyer, "Advanced iron-loss estimation for nonlinear material behavior," *IEEE Trans. Magn.*, vol. 48, no. 11, pp. 3021–3024, Nov. 2012.

[3] J. Lavers, P. Biringer, and H. Hollitscher, "A simple method of estimating the minor loop hysteresis loss in thin laminations," *IEEE Trans. Magn.*, vol. MAG-14, no. 5, pp. 386–388, Sep. 1978.

[4] S. Jacobs, D. Hectors, F. Henrotte, M. Hafner, K. Hameyer, P. Goes, D. R. Romera, E. Attrazic, and S. Paolinelli, "Magnetic material optimization for hybrid vehicle PMSM drives," presented at the Inductica Conference, CD-Rom, Chicago, IL, USA, 2009.

[5] G. Bertotti, *Hysteresis in Magnetism: For Physicists, Materials Scientists, and Engineers*. New York, NY, USA: Academic Press, 1998.

[6] G. Bertotti, A. Canova, M. Chiampi, D. Chiarabaglio, F. Fiorillo, A. M. Rietto, and G. Bertotti, "Core loss prediction combining physical models with numerical field analysis," *J. Magn. Magn. Mater.*, vol. 133, pp. 647–650, 1994.

[7] F. Fiorillo and A. Novikov, "An improved approach to power losses in magnetic laminations under non-sinusoidal induction," *IEEE Trans. Magn.*, vol. 26, no. 5, Sep. 1990.

[8] K. Yamazaki and N. Fukushima, "Iron-loss modeling for rotating machines: Comparison between Bertotti's three-term expression and 3-D Eddy-current analysis," *IEEE Trans. Magn.*, vol. 46, no. 8, Aug. 2010.